

Low-level expression of *let-7a* in gastric cancer and its involvement in tumorigenesis by targeting *RAB40C*

Qiaoyuan Yang^{1,2,†}, Zhigang Jie^{3,†}, Hong Cao⁴,
Anne R.Greenlee⁵, Chengfeng Yang⁶, Fei Zou¹ and
Yiguo Jiang^{1,2,*}

¹School of Public Health and Tropical Medicine, Southern Medical University, 18318 North Guangzhou Avenue, Guangzhou 510515, People's Republic of China, ²Institute for Chemical Carcinogenesis, State Key Laboratory of Respiratory Disease, Guangzhou Medical University, 195 Dongfengxi Road, Guangzhou 510182, People's Republic of China, ³Department of General Surgery, First Affiliated Hospital, Nanchang University, Nanchang 330006, People's Republic of China, ⁴Department of General Surgery, People's Hospital of Jiangxi Province, Nanchang 330006, People's Republic of China, ⁵The Jackson Laboratory, Bar Harbor, ME 04609, USA and ⁶Department of Physiology and Center for Integrative Toxicology, Michigan State University, East Lansing, MI 48824, USA

*To whom correspondence should be addressed. Tel: +86 20 81340186;
Fax: +86 20 81340724;
Email: jiangyiguo@yahoo.com
Correspondence may also be addressed to Fei Zou. Tel: +86 20 61648301;
Fax: +86 20 61648324;
Email: zoufei26@163.com

Gastric cancer is the fourth most common cancer and the second leading cause of cancer mortality worldwide but the underlying molecular mechanism is not entirely clear. The objective of this study was to explore the role of *let-7a* microRNA (miRNA) in gastric tumorigenesis and the possible correlation between *RAB40C* and *let-7a* miRNA in gastric cancer. We found that expression of *let-7a* is reduced in human gastric cancer tissues and cell lines and there was a significant correlation between the level of *let-7a* expression and the stage of differentiation. Overexpression of *let-7a* resulted in a decrease in cell proliferation and G₁ arrest, significantly suppressed anchorage-dependent growth *in vitro* and the tumorigenicity of gastric cancer cells in a nude mouse xenograft model. Furthermore, we demonstrated that *RAB40C* is regulated directly by *let-7a* and plays an essential role as a mediator of the biological effects of *let-7a* in gastric tumorigenesis. This study revealed that *let-7a* is significant in suppressing gastric cancer growth *in vivo* and *in vitro* and provided the first evidence that *RAB40C* is negatively regulated by *let-7a* at the posttranscriptional level via binding to the 3'-untranslated region of *RAB40C* messenger RNA in gastric cancer. The results of this study suggest that *let-7a* and *RAB40C* are potentially useful targets for gastric cancer diagnosis and therapy.

Introduction

Gastric cancer is the fourth most common cancer and the second leading cause of cancer mortality worldwide despite a decreasing incidence in recent decades (1). It remains an important public health burden worldwide, especially in developing countries. In China, gastric cancer has the highest mortality among all cancers and the overall mortality rate has increased steadily in the past 20 years (2). However, the molecular mechanisms involved in gastric cancer are diverse, complex and not fully understood.

New opportunities in the study of cancer molecular mechanisms have been provided by the discovery of microRNAs (miRNAs),

Abbreviations: CCK-8, cell counting kit-8; DMEM, Dulbecco's modified Eagle's medium; inhibitor NC, inhibitor non-specific control miRNA; mimic NC, mimic non-specific control miRNA; mRNA, messenger RNA; miRNA, microRNA; PCR, polymerase chain reaction; RT, reverse transcription; siRNA, small interfering RNA; 3'-UTR, 3'-untranslated region.

[†]These authors contributed equally to this work.

a class of short non-coding endogenous RNAs that function as negative regulators of gene expression (3). As the major endogenous triggers for posttranscriptional silencing, miRNAs can negatively regulate the expression of a protein-coding gene by binding with the 3'-untranslated regions (3'-UTRs) of their messenger RNA (mRNA) targets and then repressing expression of the target gene through mRNA degradation or translational inhibition (4,5). miRNAs are predicted to target more than one-third of human genes and each miRNA can control hundreds of target genes (6). Moreover, miRNAs have been demonstrated to be evolutionarily conserved and to perform regulatory functions in numerous biological processes, including developmental timing, cell proliferation, apoptosis, metabolism, cell differentiation and morphogenesis (7–9).

Recently acquired evidence demonstrates that miRNAs can be regulators in carcinogenesis. Calin *et al.* (10) showed that >50% of the known mature human miRNA genes are located in cancer-associated genomic regions or in fragile sites, suggesting that miRNAs might have an important role in the pathogenesis of human cancers. Moreover, different cancer types have distinct miRNA expression profiles, and an increasing number of miRNAs have been suggested to have important roles in tumor progression or in tumor suppression (11–13). Increased expressions of some miRNAs, such as *miR-21* and *miR-27a*, have been found to play crucial roles in gastric tumors (14,15). In addition, the miR-106b-25 cluster, which is upregulated in human gastric tumors, is involved in the posttranscriptional regulation of transcription factor E2F1 (16) and miR-15b and miR-16 modulate multi-drug resistance by targeting B-cell lymphoma/leukemia-2 (*BCL2*) in human gastric cancer cells (17). In contrast, *miR-9*, *miR-141*, *miR-143*, *miR-145*, *miR-433* and *miR-451* are downregulated in gastric cancer and these miRNAs act as anti-oncogenic miRNAs with a significant growth inhibitory effect on gastric cancer (18–21).

Among all human cancer-related miRNAs, the *let-7* family has attracted the most interest because its family members have been noted to express aberrantly in human cancers (22,23). The family was discovered initially in *Caenorhabditis elegans* and is currently one of the most important members of the miRNA family. The *let-7* family consists of 11 very closely related genes and many human *let-7* genes map to regions that are altered or deleted in human tumors, indicating that these genes might function as tumor suppressors (22). Moreover, when overexpressed in colon cancer cells, *let-7* miRNA leads to growth proliferation associated with a reduced level of *RAS* protein (24). *let-7a* is downregulated in Burkitt's lymphoma and it has been shown to be an anticancer miRNA that repressed *C-MYC* expression at the translational level (25). Recently, the implication of *let-7* in carcinogenesis has been extended to the repression of high-mobility group A2, thus preventing oncogenic transformation in many tumors (26,27). These findings suggest that *let-7* miRNAs participate actively in tumorigenic processes and the targets involved in the regulation of *let-7* miRNAs have been associated with various tumorigenic processes in addition to the miRNAs themselves. However, the data for the relationship between gastric carcinogenesis and the expression of *let-7a* miRNA are very limited. Evidence collected to date shows *let-7a* was linked to the modulation of different target genes, the most well-known being the *RAS* family. The *RAS* proteins function as the critical molecular switch for various signaling pathways controlling the diverse biological processes. *RAB40C* is a member of the *RAS* family, which plays important roles in tumorigenesis. With the help of a bioinformatic analysis, we found *RAB40C* contained the *let-7a* binding site and was evolutionarily conserved across 10 species. To our knowledge, there is no report of work investigating the role of *let-7a* or a possible correlation between *RAB40C* and *let-7a* miRNA in gastric cancer.

In this study, we used the quantitative real-time polymerase chain reaction (PCR) to examine the expression of *let-7a* mature miRNA in 27 matched pairs of normal and gastric cancer tissues from patients. In comparison with normal tissues, we found that the expression of *let-7a* was significantly lower in gastric tumor specimens. Importantly, increased expression of *let-7a* suppressed cell growth *in vitro* and tumor growth *in vivo* and was associated with decreased rates of cell proliferation and the cell cycle. This is the first report that *let-7a* is involved in tumorigenesis of gastric cancer both *in vitro* and *in vivo*. Furthermore, it is confirmed for the first time that *let-7a* targets *RAB40C* directly. By targeting *RAB40C*, *let-7a* suppresses proliferation and anchorage-independent growth of human gastric cancer cells. Our findings suggest that *let-7a* and *RAB40C* might be valuable tools for developing interventions aimed at treating and diagnosing gastric cancer.

Materials and methods

Patients and tissue samples

In 2008–09, 27 pairs of gastric cancer tissues and matched normal gastric tissues were obtained with informed consent from patients in the First Affiliated Hospital of Nanchang University (Nanchang, China). All tissue samples were confirmed histopathologically and snap-frozen in liquid nitrogen. The non-cancerous gastric tissues were taken 3 cm away from the tumor. Clinicopathologic information was available for all samples and the study was approved by the Medical Ethics Committee of Nanchang University and the Medical Ethics Committee of Guangzhou Medical University.

Cell lines and reagents

The human gastric epithelial cell line GES-1 and human gastric cancer cell lines SGC-7901, BGC-823 and HGC-27 were purchased from the Cell Resource Center of XiangYa Central Laboratory (Changsha, China). Human gastric cancer cell line MKN-28 was provided by the Laboratory Animal Center of the Fourth Military Medical University (Xian, China). Human gastric cancer cell line AGS was donated by the Sun Yat-Sen University Cancer Center (Guangzhou, China). All cells, except AGS cells, were grown in Dulbecco's modified Eagle's medium (DMEM) (Gibco, Carlsbad, CA) supplemented with 10% (vol/vol) fetal bovine serum, 50 U/ml penicillin and 50 µg/ml streptomycin. The AGS cells were grown in F12k medium (Sigma, Louis, MO) supplemented with 10% fetal bovine serum, with 50 U/ml penicillin and 50 µg/ml streptomycin. All cell lines were incubated at 37°C in a humidified 5% (vol/vol) CO₂ atmosphere.

RNA extraction and quantitative real-time-PCR-based detection of *let-7a* and *RAB40C* mRNA

Total RNA from tissue samples and cell lines was obtained with the TRIzol® isolation reagent (Invitrogen, Carlsbad, CA) following the manufacturer's instructions. About 100 mg of tissue was homogenized in 1 ml of TRIzol reagent and then entered into the same step of the analysis as cell samples. The concentration, purity and amount of total RNA were determined by ultraviolet spectrometry (ND-1000 spectrophotometer; NanoDrop Technologies, Wilmington, DE).

The reverse transcription (RT)-PCR was used to detect the expression of *let-7a* and the *RAB40C* gene at the transcript level as described (28). Briefly, this method uses two-step RT-PCR. In the RT step, complementary DNA was reverse transcribed from total RNA samples using the ReverTra Ace qPCR RT kit (TOYOBO, Tokyo, Japan). The quantitative real-time-PCR for detecting the expression of *let-7a* using the TaqMan MicroRNA assay (Applied Biosystems, Foster City, CA) together with the TaqMan Universal PCR Master Mix (Applied Biosystems) were done with an Applied Biosystems 7500 real-time PCR system (Applied Biosystems). The relative quantification of *let-7a* was calculated using the 2^{-ΔΔC_t} method normalized with respect to *RNU6B* as the internal control and relative to a calibrator sample as the external control. The SYBR Premix Ex Taq™ Kit (TaKaRa, Dalian, China) was used for detecting the expression of *RAB40C* mRNA following the manufacturer's instructions. The data were also calculated using the 2^{-ΔΔC_t} method normalized to the individual β-actin level. All primers were synthesized by TaKaRa. The primers were β-actin forward: CCCAGATCATGTTTGAGACCT and reverse: GAGTCCATCACGATGC-CAGT and *RAB40C* forward: TCATCGACAAGCTTCCACTG and reverse: TTGGACCTCTTGAGGCTGTT.

miRNA and small interfering RNA transfections

The *let-7a* mimic was an RNA duplex with the sequence: 5'-UGAGGUA-GUAGGUUGUAUAGUU-3' and 5'-CUAUACAACCUACUACCUCAUU-3'.

The mimic non-specific control miRNAs duplex (named mimic NC) with a sequence of: 5'-UUCUCCGACGUGUCACGUTT-3' and 5'-ACGUGA-CACGUUCGGAGAATT-3' was not homologous to any human genome sequence. For the *in vivo* tumorigenicity assay, all pyrimidine nucleotides in

the *let-7a* mimic or mimic NC were substituted by their 2'-*O*-methyl analogs to improve RNA stability. The anti-*let-7a*: 5'-AACUAUACAACCUACUAC-CUCA-3' was a 2'-*O*-methyl-modified oligoribonucleotide designed as *let-7a* inhibitor. The inhibitor non-specific control miRNAs (named inhibitor NC), with the sequence: 5'-CAGUACUUUUGUGUAGUACAA-3' was used as a negative control for anti-*let-7a* in the antagonism experiment. All the RNA oligoribonucleotides were purchased from GenePharma (Shanghai, China). A blank control treated with only the transfection reagent was used in every transfection experiment. Small interfering RNAs (siRNAs) for human *RAB40C* sequence sense: 5'-GGGACAUUGACCACUCAAATT-3' and antisense: 5'-UUUGAGUGGUCAAUGUCCCTT-3' and scrambled siRNA were designed and synthesized by GenePharma.

Cells were seeded onto six-well plates (3 × 10⁵ cells per well) the day before transfections were performed. Cells (~60% confluent) were transfected with *let-7a* mimic (50 nmol/L), mimic NC (50 nmol/L), inhibitor (100 nmol/L) or inhibitor NC (100 nmol/L) using Lipofectamine™ 2000 (Invitrogen) and transfection efficiency (>90%) was confirmed with the use of the Silencer 5-carboxyfluorescein-labeled Negative Control (GenePharma). For the miRNA and siRNA combination experiments, cells were transfected with *let-7a* mimic (50 nmol/L) for 24 h. These cells were then cotreated with *RAB40C* siRNA (100 nmol/L) or siRNA NC (100 nmol/L) for another 24 h. Total RNA and protein were prepared 1 or 2 days after transfection and were used for RT-PCR or western blot analysis to validate the knockdown efficiency.

Cell proliferation assay

The cell proliferation assay was done with a cell counting kit-8 (CCK-8; Dojindo, Tokyo, Japan) at 24 h after transfection. Briefly, 5000 transfected GES-1, AGS or BGC-823 cells were plated per well in 96-well plates at 24 h after transfection and cultured in 100 µl of cell culture medium per well for 24 h in normal conditions. After incubation for 24 h, 20 µl of CCK-8 reagent was added to each well and incubated at 37°C for 1 h. The absorbance at 450 nm (A₄₅₀) and at 650 nm (A₆₅₀) were measured with a Synergy 2 microplate reader (BioTek, Winooski, VT). The final absorbance was calculated as A₆₅₀ - A₄₅₀, and cell viability was normalized as:

$$(\text{Final absorbance treated/final absorbance control}) \times 100\%.$$

Colony formation assay

Transfected GES-1, AGS and BGC-823 cells were trypsinized, counted and seeded at a density of 1000 cells per 60 mm culture dish in normal culture medium for colony formation assay and incubated for 10 days at 37°C in a humidified 5% CO₂ atmosphere. During colony growth, the culture medium was replaced every 3 days and a colony was counted only if it contained >50 cells. Colony formation and growth were visualized by staining with crystal violet and the colony formation rate was calculated as:

$$(\text{Number of colonies/number of seeded cells}) \times 100\%.$$

Cell cycle analysis

Cells were harvested at 24 h after transfection and fixed in 70% ice-cold ethanol, treated with RNase A, stained with 50 mg/ml propidium iodide and 0.1 mg/ml RNase A for DNA content analysis by flow cytometry with a FACS Calibur system (Becton Dickinson, Franklin, NJ). The percentage of cell population in each phase was calculated with FlowJo FACS analysis software (Tree Star, Ashland, OR).

Soft agar assay

Soft agar plates were prepared in triplicate in 60 mm dishes with a bottom layer of 0.6% (wt/vol) Noble agar (Sigma) in serum-free DMEM. Thereafter, transfected cells were trypsinized and 1000 cells per dish were seeded onto the bottom agar layer after mixing with 0.3% Noble agar in DMEM supplemented with 10% fetal bovine serum and allowed to harden. To assess cell viability before plating in soft agar, the number of cells was determined by staining with trypan blue. The dishes were incubated for 3 weeks at 37°C in a humidified 5% CO₂ atmosphere and scored for clones. The result is expressed as the number of colonies containing at least 50 cells per well.

Tumorigenicity assays in nude mice

Five-week-old Balb/c nude mice were provided by Guangzhou University of Traditional Chinese Medicine (Guangzhou, China). All experimental procedures involving animals were in accordance with the Guide for the Care and Use of Laboratory Animals and were in accord with the institutional ethical guidelines for experiments with animals. Transfected and control BGC-823 cells were trypsinized, collected by centrifugation and suspended in DMEM.

A 0.2 ml sample of culture medium containing 5×10^6 cells was injected subcutaneously into the right-hand side of the posterior flank of each mouse. The mice were housed in a pathogen-free environment and monitored every 5 days for tumor growth. The mice were killed after 40 days and the weight and volume of each tumor were determined. The tumor xenografts were excised and weighed, then used for the extraction of total RNA and immunohistochemical assays. The tumor latency time was determined as the time to appearance of palpable tumor and the volume (V) was calculated as described (29).

Immunohistochemistry

Ki-67 protein expression in the cancer tissues of nude mice was detected using the streptavidin-peroxidase complex method with a Histostain-plus kit (Zhongshan Golden Bridge Biotechnology, Beijing, China). Rabbit anti-human Ki-67 antibodies (Boster, Wuhan, China) were used at a dilution of 1:400 as primary antibodies. Color development was achieved with 3',3'-diaminobenzidine, which stained positive cells brown. Normal rabbit serum and secondary antibody alone were used as negative controls.

Western blotting

Total proteins were prepared by standard procedures and quantified by the BCA method (Jiancheng, Nanjing, China). A 20 μ g sample of protein was mixed with $5 \times$ sodium dodecyl sulfate/polyacrylamide gel electrophoresis sample buffer (Weijia, Guangzhou, China) and boiled for 5 min before sodium dodecyl sulfate-polyacrylamide gel electrophoresis (15% polyacrylamide gel) and transfer to a polyvinylidene difluoride membrane (Millipore Corp., Bedford, MA). The membrane was blocked with 5% non-fat dry milk in phosphate-buffered saline for 45 min at 37°C with agitation. RAB40C protein and glyceraldehyde-3-phosphate dehydrogenase on the same membrane were quantified by dividing the membrane into two pieces according to the molecular mass of prestained protein standards (Weijia). The piece of the membrane with the greater molecular mass proteins was incubated with a primary antibody for rat anti-human RAB40C (Epitomics, Burlingame, CA) at a concentration of 1:1000 at 37°C for 1 h. The other piece of the membrane was incubated with a primary antibody for mouse anti-human glyceraldehyde-3-phosphate dehydrogenase (Epitomics) at a concentration of 1:1500. Signals were detected by secondary antibodies labeled with IRDye 800 (Rockland Immunochemicals, Gilbertsville, PA) and signal intensity was determined with an Odyssey Infrared Imaging System (Li-Cor Biosciences, Lincoln, NE).

Luciferase reporter assay

The full-length 3'-UTR of RAB40C gene (GenBank accession number NM_021168; length 1650 bp) was amplified from GES-1 cells complementary DNA and cloned into the NotI and XhoI sites in a psiCHECK-2 vector (Promega, Madison, WI) downstream of the reporter gene. The primers for RAB40C were forward: 5'-AGCTTTGTTTAAACCGGGATGGGCGCGGGGATG-3' and reverse: 5'-AGCTTTGTTTAAACTGTGGGGACCACAGCTGAAT-TAC-3'. To introduce mutations into let-7a target sites in the RAB40C coding region, primers were designed for site-directed mutagenesis based on wild psiCHECK-2-RAB40C 3'-UTR plasmid that resulted in the destruction of the let-7a target site without altering the amino acid sequence of RAB40C. The sites were mutated as follows: before mutagenesis, CUACCUC; after mutagenesis, AUCGAGC. The primers for RAB40C mt were forward: 5'-CA-CAGCACTGGTGATCACCTATCGCTCCTGTCTCAGGCCGTGCGGC-3' and reverse: 5'-GCCGCACGGCCTGAGGACAGGATCGATAGGTGAG-CACCAGTGTGTG-3'. The segment of the RAB40C 3'-UTR containing the mutated let-7a target sequence, was also cloned into the psiCHECK-2 Luciferase vector (Promega). The resulting wild and mutated RAB40C expression vectors were confirmed by sequencing. The construct of reporter vector was performed by Landbiology (Guangzhou, China).

For the luciferase reporter assay, GES-1 cells (50% confluent in 24-well plates) were cotransfected with 0.5 μ g of psiCHECK-2 vector constructs with or without 20 μ M let-7a mimic or inhibitor for 48 h by Lipofectamine 2000 (Invitrogen). At 48 h after transfection, the activity of Renilla luciferase and firefly luciferase was measured with the Dual-luciferase Reporter Assay System (Promega). Relative luciferase activity was normalized with firefly luciferase activity and then compared with the psiCHECK-2 vector control.

Statistical analysis

All statistical analysis was done with SPSS13.0 software. Values are expressed as mean \pm SD. Differences between groups were analyzed by Student's t -test or the non-parametric Mann-Whitney U -test for comparison of two groups and one-way analysis of variance or the non-parametric Kruskal-Wallis H test for multiple comparisons. Nonlinear regression analysis between groups was used with logarithmic regression model by method of curve estimation. All experiments were done at least in triplicate and the level of statistical significance was set at $P < 0.05$ for all tests.

Results

Expression of let-7a is reduced in human gastric cancer tissues and cell lines

The clinicopathologic data for 27 patients are given in Table I. Based on the results of TaqMan real-time PCR, we found the expression of let-7a in 21 cancer tissues was lower than that in the matched normal tissues (Figure 1A). The expression of let-7a was significantly lower in gastric cancer tissues than that in normal tissues, with a median change of 0.38-fold (Figure 1B). Next, we examined the correlation of the tumor tissue (T)/normal tissue (N) ratios for let-7a expression with the clinicopathologic factors given in Table 1. The T/N ratios in patients with poor differentiation were significantly lower than those with moderate or good differentiation (Table 1; Figure 1C). However, there was no significant difference between the groups divided by any other clinicopathologic feature, including gender, tumor size, histologic cell type, lymph node metastasis or venous invasion. To confirm the association between the expression of let-7a and gastric cancer, five cell lines derived from gastric cancers with various degrees of differentiation were selected to detect let-7a expression: MKN-28 (well differentiated), AGS (well differentiated), SGC-7901 (moderately differentiated), BGC-823 (poorly differentiated or undifferentiated) and HGC-27 (undifferentiated). The data showed that the expression of let-7a was significantly downregulated in MKN-28 (0.63-fold), AGS (0.33-fold), SGC-7901 (0.28-fold), BGC-823 (0.23-fold) and HGC-27 (0.13-fold) cells compared with normal human gastric epithelial cell line GES-1 (Figure 1D).

let-7a regulates cell proliferation and the cell cycle

We evaluated the transfection efficiency by determining the percentage of cells containing the 5-carboxyfluorescein-labeled non-specific miRNA control and the results indicated successful transfection of 5-carboxyfluorescein-labeled non-specific miRNA control into >90% of cells of all the cell lines used in this study. TaqMan real-time PCR revealed the transfected let-7a mimic significantly increased the levels of let-7a (Figure 2A), whereas the transfected let-7a inhibitor effectively inhibited the expression of let-7a (Figure 2B) compared with mimic NC or inhibitor NC cells or with untransfected cells in all six cell lines, which demonstrated that the transfected let-7a mimic and inhibitor were functional.

Table I. The Clinicopathologic factors of 27 gastric cancer patients and comparison of let-7a expression in different groups

Clinicopathologic factor	No. of patients	Relative let-7a expression Min-max (median)	P
Age (years)			
>60	19	0.04–8.97 (0.47)	0.313
≤60	8	0.08–2.00 (0.25)	
Gender			
Male	17	0.04–8.97 (0.47)	0.335
Female	10	0.04–2.63 (0.25)	
Tumor size (cm)			
>3	7	0.10–2.72 (0.82)	0.580
≤3	20	0.04–8.97 (0.31)	
Histologic cell type			
Well differentiated	6	0.10–8.97 (2.06)	0.018
Moderately differentiated	8	0.16–2.63 (0.45)	
Poorly differentiated	13	0.04–2.00 (0.19)	
Lymph node metastasis			
Absent	12	0.04–2.72 (0.51)	0.727
Present	15	0.04–8.97 (0.35)	
Venous invasion			
Absent	9	0.04–8.97 (0.20)	0.862
Present	18	0.04–2.72 (0.49)	

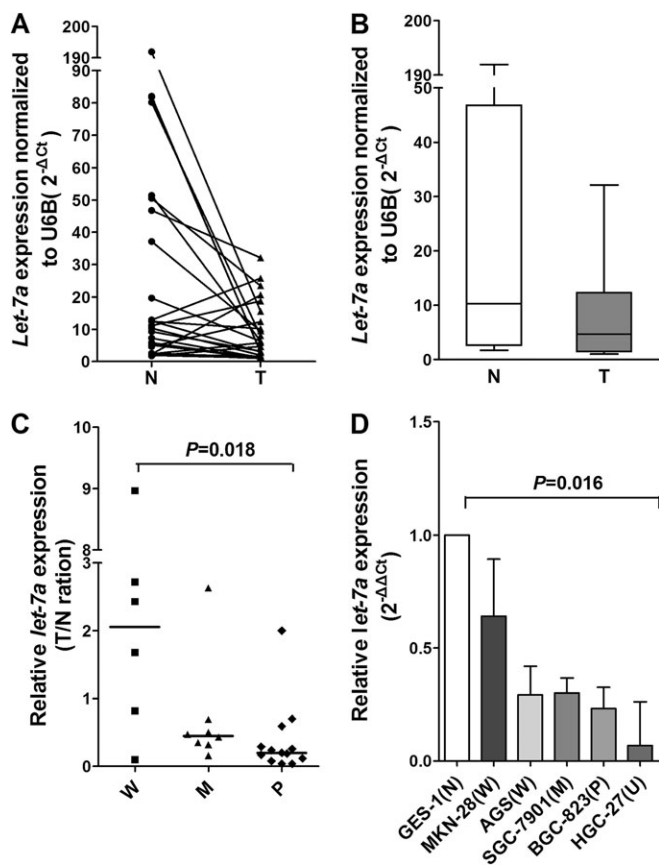


Fig. 1. Level of expression of mature *let-7a* in gastric cancer tissue specimens and cell lines. Mature *let-7a* expression was analyzed by TaqMan real-time PCR and normalized to *U6B* expression. (A) The comparison of *let-7a* expression between matched normal gastric and gastric cancer tissues in 27 patients. T, gastric cancer tumor tissue; N, pair-matched adjacent non-tumor tissue. (B) The data for *let-7a* expression were analyzed using the Mann–Whitney *U*-test. (C) The ratios of tumor to normal tissue for *let-7a* expression are presented as the relative tumor tissue/normal tissue ratio (T/N ratio) of *let-7a* expression. The T/N ratios were analyzed statistically in patients of different pathological grade (Kruskal–Wallis *H* test, $P = 0.018$). Horizontal lines show the median value of each group. W, well differentiated; M, moderately differentiated; P, poorly differentiated. (D) The expression of *let-7a* in five gastric cancer cell lines relative to the normal gastric cell line GES-1 (Kruskal–Wallis *H* test, $P = 0.016$). N, normal gastric epithelial cell line; W, well differentiated cancer cell line; M, moderately differentiated cancer cell line; P, poorly differentiated cancer cell line; U, undifferentiated cancer cell line. The data are shown as median with interquartile range for three independent experiments.

We used the CCK-8 assay to measure cell proliferation *in vitro*. The AGS and BGC-823 cell lines, which had the highest level of *let-7a* expression and the smallest standard deviation (Figure 2A), were used in an overexpression study. AGS and BGC-823 cells transfected with the *let-7a* mimic showed a significant reduction in the number of metabolically active cells compared with those transfected with mimic NC or the untransfected control (Figure 2C). The GES-1 cell line, which had the lowest level of *let-7a* expression (Figure 2B), was used for an inhibition study. An increase of 58.8% in cell growth was observed in GES-1 cells after transfection with a *let-7a* inhibitor compared with inhibitor NC (Figure 2C).

As shown in Figure 2D, DNA content analysis by flow cytometry revealed *let-7a* restoration induced an accumulation of AGS cells in the percentage of cells at the G_1 phase from 55.38 to 64.87% and a reduction of cells in S phase from 37.94 to 26.55% compared with the mimic NC group and this effect on cell cycle was observed also for BGC-823 cells (Figure 2E). In contrast, the percentage of GES-1 cells transfected with *let-7a* inhibitor in the G_1 phase was decreased from

75.01 to 60.35%, whereas the percentage of cells in the S phase was increased from 20.61 to 35.76% compared with the inhibitor NC group (Figure 2F). These findings, together with the cell proliferation results (Figure 1C), illustrated that *let-7a* could be a tumor suppressor gene in gastric cancer.

let-7a suppresses anchorage-dependent growth *in vitro* and tumor growth *in vivo*

The significant reduction of *let-7a* on cell growth *in vitro* prompted us to explore the possible biological significance of *let-7a* in tumorigenesis. AGS and BGC-823 cells were used in these assays. To test how long the promotion of *let-7a* by the *let-7a* mimic could be sustained, we measured the *let-7a* levels after 1, 2, 3, 4, 7, 10, 14 and 21 days from transfection by TaqMan real-time PCR. We found that the promotion effect lasted up to at least 10 days in *let-7a* mimic-transfected AGS cells (Figure 3A) and 14 days in *let-7a* mimic-transfected BGC-823 cells (Figure 3B) compared with mimic NC-transfected cells. The colony numbers of AGS and BGC-823 cells that formed in soft agar medium were decreased at 3 weeks after transfection with the *let-7a* mimic (Figure 3C and D). Furthermore, AGS and BGC-823 cells transfected with the *let-7a* mimic displayed fewer and smaller colonies compared with the mimic NC-transfected and untransfected cells (Figure 3E). Taken together, these results suggest that the initial promotion of *let-7a* might be sufficient to inhibit tumor growth and prompted us to investigate the role of *let-7a* on tumor growth *in vivo*.

Poorly differentiated BGC-823 cells were included in this step to further confirm the promotion effect on tumor growth *in vivo* induced by transfection of the *let-7a* mimic. The emerging rate of tumor and tumor latency time showed a significant difference between the mice injected with *let-7a* mimic-transfected cells and the mimic NC group (Figure 4A). It is of considerable interest that tumors derived from cells transfected with the *let-7a* mimic grew substantially more slowly than the mimic NC group throughout tumor growth (Figure 4B). The average weight of tumors derived from cells transfected with the *let-7a* mimic was only 63.2% of that derived from the cells transfected with the mimic NC (Figure 4C and D). There was no significant difference of tumor volume, tumor average weight or other indices between the mimic NC-transfected cell group and the untransfected cell group. Additionally, the expression of the proliferation marker Ki-67 was significantly lower in tumor xenografts of the *let-7a* mimic group compared with the mimic NC and untransfected groups (Figure 4E). These results indicate that the reduced tumor growth is probably to be due to decreased proliferation induced by *let-7a*.

RAB40C is a direct target of *let-7a*

A bioinformatic analysis identified *RAB40C* as a hypothetical target gene of *let-7a*, as identified by TargetScan algorithms (<http://www.targetscan.org>). The *let-7a* targeting sites in *RAB40C* 3'-UTR are conserved among mammals and the corresponding sequences of the *RAB40C* mutated 3'-UTRs are shown in supplementary Figure S1, available at *Carcinogenesis* Online. The putative secondary RNA hybrid (<http://bibiserv.techfak.uni-bielefeld.de/rnahybrid/>) for human *let-7a* and *RAB40C* or *N-Ras* mRNA with minimal free energy is shown in supplementary Figures S2 and S3, available at *Carcinogenesis* Online. Our analysis indicates that *let-7a* has a more stable secondary structure with lower free energy with *RAB40C* compared with the validated target *N-Ras*.

Next, we found overexpression of *let-7a* in AGS and BGC-823 cells effectively decreased the level of the *RAB40C* protein. A blocking strategy was further adapted by introducing the *let-7a* inhibitor into GES-1 cells, which increased the level of the *RAB40C* protein (Figure 5A). In both cases, neither the *let-7a* mimic nor the inhibitor affected the mRNA of *RAB40C* (supplementary Figure S4 is available at *Carcinogenesis* Online), suggesting posttranscriptional regulation of *RAB40C* by *let-7a* in gastric cancer cell lines. A further hint about the potential role of *let-7a* in the regulation of *RAB40C* expression came from the analysis of five different gastric cancer cell lines (MKN-28, AGS, SGC-7901, BGC-823 and HGC-27) that showed

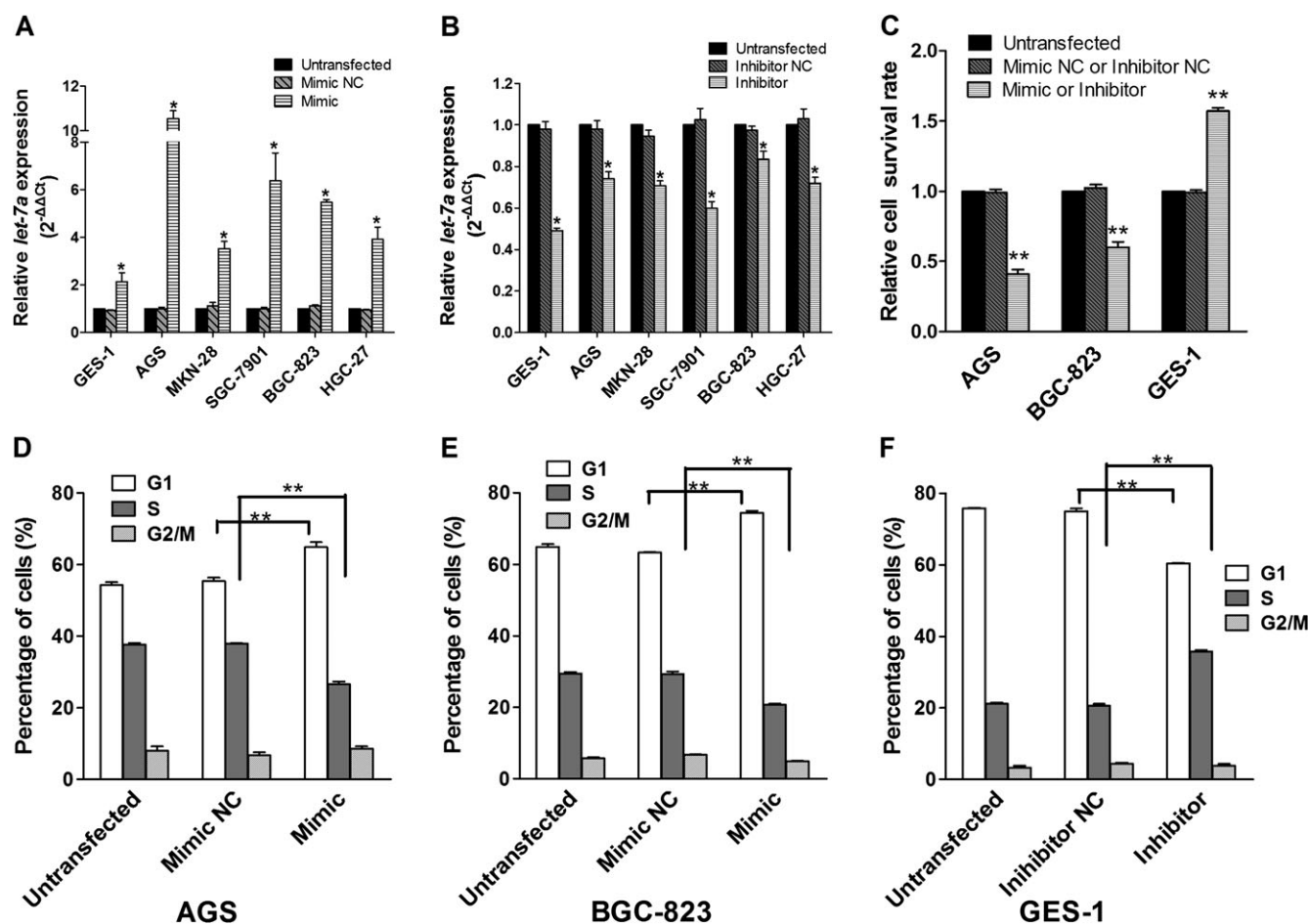


Fig. 2. Expression of *let-7a* after transfection with the *let-7a* mimic or inhibitor in six gastric cell lines and overexpression or knockdown of *let-7a* in gastric cells affected cell growth *in vitro*. Total RNA was isolated 24 h after transfection for the detection of *let-7a* and mature *let-7a* expression was analyzed by TaqMan real-time PCR and normalized to U6B expression. (A) Expression of *let-7a* in *let-7a* mimic-transfected, mimic NC-transfected and untransfected gastric cells. (B) Expression of *let-7a* in *let-7a* inhibitor-transfected, inhibitor NC-transfected and untransfected gastric cells. (C) Overexpression or knockdown of significant *let-7a*-affected cell proliferation in AGS, BGC-823 or GES-1 cells as measured by the CCK-8 assay. (D and E) Overexpression of *let-7a* resulted in G₁ arrest in AGS (D) and BGC-823 (E) cells. (F) Knockdown of *let-7a* enhanced S phase cells in GES-1 cells. (A-F) The data are shown as mean \pm SD for three independent experiments, each done in triplicate. * $P < 0.05$, ** $P < 0.01$, compared with the *let-7a* mimic NC- or inhibitor NC-transfected group or with untransfected group. P values were obtained by one-way analysis of variance or the non-parametric Kruskal-Wallis H test for multiple comparisons.

a significant reversed nonlinear correlation between *let-7a* levels and the *RAB40C* protein (Figures 5B and C). To assess the clinical relevance of these findings, we examined the correlation between the level of the *RAB40C* protein with *let-7a* expression in the 27 matched normal and cancer tissues (Figure 5D). There was a reversed nonlinear correlation between the level of the *RAB40C* protein and *let-7a* expression (Figure 5E). These results support the premise that down-regulation of *let-7a* increases the level of *RAB40C* gene in gastric cancer.

To confirm the direct interaction between *let-7a* and its binding site within *RAB40C* mRNA, a human *RAB40C* 3'-UTR fragment containing a wild type or mutant *let-7a*-binding sequence was cloned downstream of the luciferase reporter gene. The psiCHECK-2 vector was cotransfected in GES-1 cells in association with *let-7a* mimic or inhibitor. GES-1 cells transfected with psiCHECK-2 vector showed ~50% decrease or 30% increase of the relative luciferase activity when cotransfected with *let-7a* mimic or inhibitor (Figure 5F and G). The *let-7a* seed sequence was mutagenized in the cloned *RAB40C* 3'-UTR region to generate the psiCHECK-2-*RAB40C* mt vector. No significant change of the relative luciferase activity was observed following the cotransfection of this mutagenized vector with *let-7a* mimic or inhibitor (Figure 5F and G). These findings showed a direct interaction between *let-7a* and *RAB40C* mRNA and indicated that *let-7a* might suppress gene expression through the *let-7a* binding sequence at the 3'-UTR of *RAB40C*.

RAB40C mediates the *let-7a* effect on cell proliferation and anchorage-independent growth

To confirm that the *let-7a* effect on cell proliferation and anchorage-independent growth is associated with its modulation of *RAB40C*, GES-1 cells were transfected with siRNA targeting *RAB40C* or control siRNA. Transfection of AGS cells with siRNA for *RAB40C* effectively suppressed *RAB40C* mRNA expression (Figure 6A) and *RAB40C* protein (Figure 6B). A similar effect was observed in BGC-823 cells (Figure 6A and B). *RAB40C* depletion significantly alleviated the anti-proliferative effect of *let-7a* upregulation in AGS cells and BGC-823 cells as determined by the CCK-8 assay (Figure 6C). Furthermore, *RAB40C* siRNA attenuated the plating efficiency of cells in soft agar, which was decreased upon the transfection of *let-7a* mimic in AGS cells and BGC-823 cells (Figure 6D). These data provided further evidence that *RAB40C* was targeted by *let-7a* and therefore suggested that *RAB40C* mediates the *let-7a* effect on cell proliferation and anchorage-independent growth in gastric cancer cells.

Discussion

miRNAs are becoming increasingly recognized as regulatory molecules in human cancers, which have been demonstrated to function as oncogenes or tumor suppressors. *let-7a* has been suggested to function as a tumor suppressor and have a strong correlation with

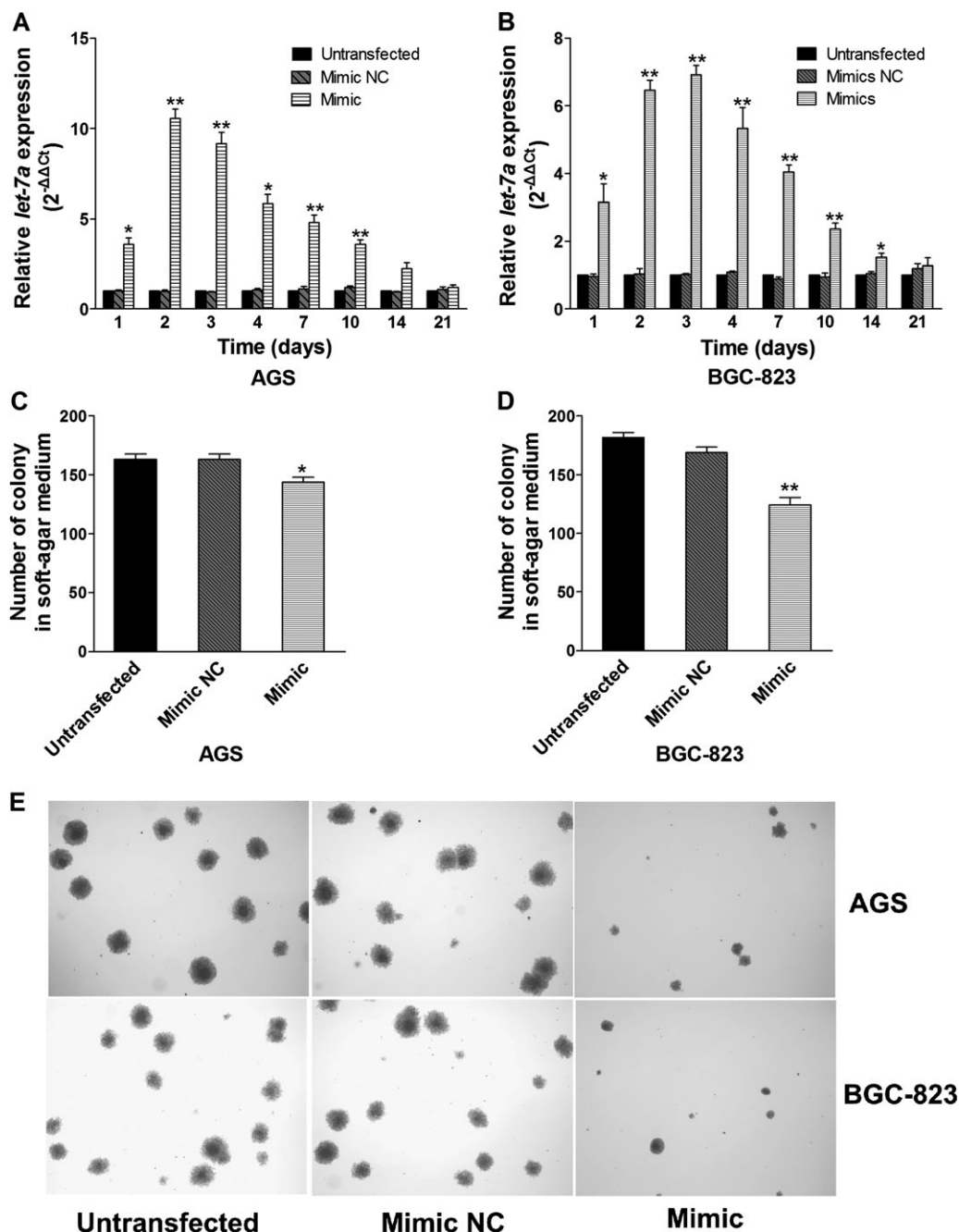


Fig. 3. The change of *let-7a* expression and inhibition of anchorage-dependent growth by overexpression of *let-7a*. (A and B) The change of *let-7a* expression after 1, 2, 3, 4, 7, 10, 14 and 21 days from *let-7a* mimic and *let-7a* mimic NC transfected or untransfected AGS (A) or BGC-823 (B) cells. (C and D) Inhibition of anchorage-dependent growth by the *let-7a* mimic in AGS (C) and BGC-823 (D) cells. (E) Representative results of colony formation of untransfected, NC-transfected and mimic-transfected AGS and BGC-823 cells. The data in (A–D) are shown as mean \pm SD from three independent experiments. * $P < 0.05$; ** $P < 0.01$, compared with the *let-7a* mimic NC-transfected group. P values were obtained by one-way analysis of variance or the non-parametric Kruskal–Wallis H test for multiple comparisons.

clinicopathologic factors or prognosis in cancer patients (22,23,30). In the present study, the 75% *let-7a* expression of gastric carcinoma samples was significantly lower than that of matched normal tissues, suggesting that reduced *let-7a* expression is a frequent event in gastric cancer. Furthermore, we found that the expression level of *let-7a* was associated with the differentiation stage in patients and the same results were observed in the cells. Our analytical results showed that tumor tissue of patients and cell lines with lower levels of *let-7a* tended to have poor differentiation. This observation was consistent with an earlier report that identified the loss of *let-7* expression as a marker for less differentiated cancer (31). These

results indicated that *let-7a* expression might be an important indicator for gastric cancer diagnosis and clinical stage.

miRNAs have been shown to be important in the development and maintenance of normal cellular function, and alteration in expression of miRNAs can result in human cancer initiation and tumor progression. Some studies have reported that *let-7* miRNA was a master regulator of cell proliferation and cell cycle pathways in lung, colorectal and hepatic cells (22,23,32). However, no information is available on the impact of altered *let-7a* expression on gastric cancer cell proliferation pathways. Here, we show that overexpression of *let-7a* resulted in 40–50% decrease in cell proliferation rate and the effect

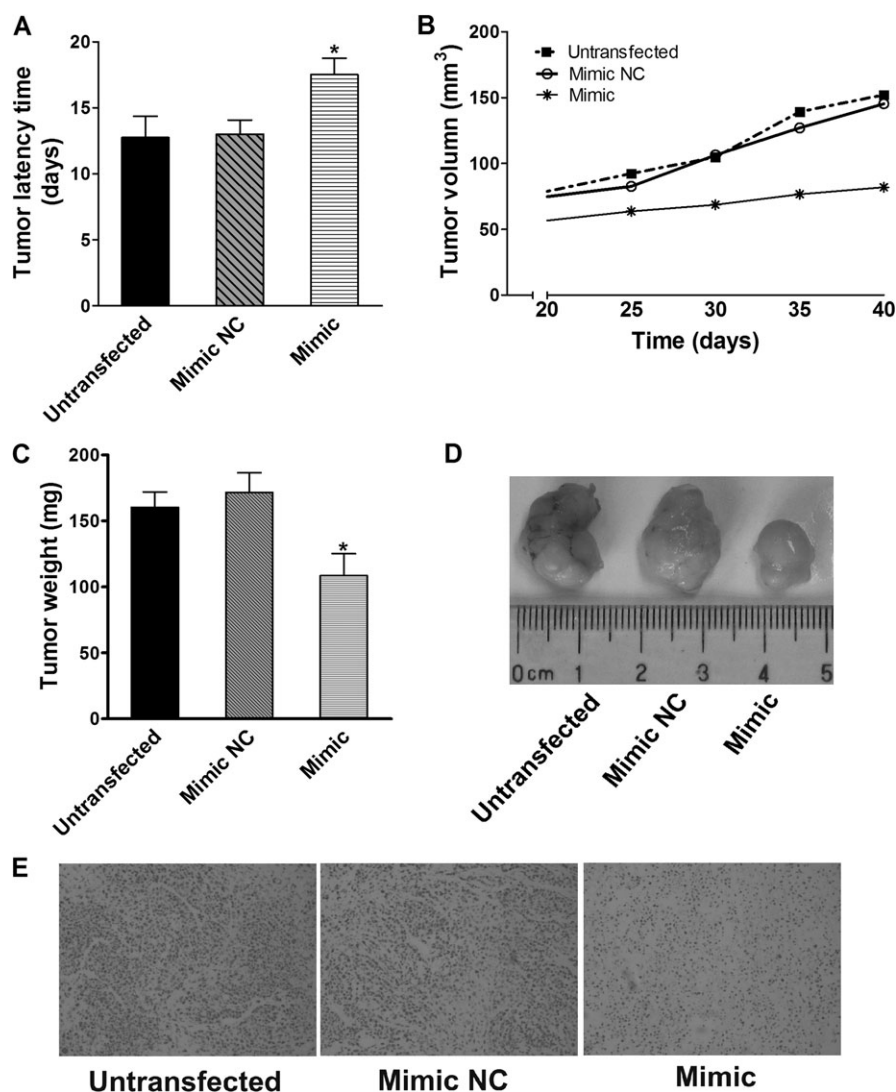


Fig. 4. Suppression of tumor growth by overexpression of *let-7a*. (A) The tumor latency was the number of days to the onset of palpable tumor and the values are given as mean \pm SD ($n = 4$ per group). * $P < 0.05$, compared with *let-7a* mimic NC-transfected or untransfected cells-injected group. (B) Tumor growth curves were measured after injection of untransfected BGC-823 cells, *let-7a* mimic NC and *let-7a* mimic-transfected BGC-823 cells. The tumor volume V (in cubic centimeter) was calculated using the formula volume $V = 0.5 L W^2$, where L is the length of the tumor (in centimeter), W is the width of the tumor (in centimeter) and V is the mean tumor volume ($n = 4$ per group). (C) Tumor weight; the values are given as mean \pm SD ($n = 4$ per group). * $P < 0.05$, compared with *let-7a* mimic NC-transfected cells-injected group. (D) Effect of *let-7a* on tumorigenesis *in vivo*. The photograph shows representative features of tumor xenografts 40 days after inoculation. (E) Representative immunohistochemical assay of Ki-67 in tumor xenografts of mice injected with untransfected cells, mimic NC-transfected cells or *let-7a* mimic-transfected cells. P values were obtained by one-way analysis of variance for multiple comparisons.

of *let-7a* was attenuated by the inhibition of *let-7a*. More importantly, decreased levels of protein Ki-67, which has been used as a marker for cell proliferation (33), were detected in the xenografts of the *let-7a* mimic-transfected cells. It further confirmed that cell proliferation was affected by *let-7a* miRNA in gastric cancer. Flow cytometry-based cell cycle analysis revealed a trend toward an accumulation of cells in G_1 phase in *let-7a* mimic-transfected gastric cancer cells. Conversely, *let-7a* inhibitor caused a significant increase in the fraction of cells in S phase. However, in the present study, we did not observe any apparent increase of the sub- G_1 population or any apoptosis-related morphological changes, such as nuclear blebbing or condensation, under the phase contrast microscope (data not shown). This suggests that growth suppression induced by *let-7a* transfection was caused by induction of G_1 arrest rather than apoptosis. This study confirmed the results of that earlier work and extended our knowledge of the inhibitory effect of *let-7a* on cell proliferation and cell cycle control in gastric cancer cells. All the results demonstrated that the consistently reduced *let-7a* expression in gastric cancer should be

a factor contributing to the development of the tumor rather than being affected as a consequence of the disease.

Gastric tumor xenograft models were established to investigate the antitumor effect of *let-7a* *in vivo* relevant to our findings *in vitro*. Mice injected with BGC-823 cells transfected with the *let-7a* mimic showed a significant inhibition of tumor xenografts, implying that overexpression of *let-7a* suppressed tumor growth of gastric cancer significantly in nude mice. Therefore, therapeutic strategies to introduce *let-7a* into cancer cells might be useful for retarding the process of tumorigenesis. Experiments with the xenograft carcinoma model indicated that one transient transfection with *let-7a* mimic is sufficient to cause substantial inhibition of tumor growth, which raises the possibility that *let-7a* mimic might have potential therapeutic value, consistent with the earlier studies (34).

It is generally accepted that miRNAs exert their function through regulating the expression of their downstream target genes (35). Thus, putative *let-7a* targets were predicted using TargetScan programs. Computational predictions suggest that *let-7a* can target 819

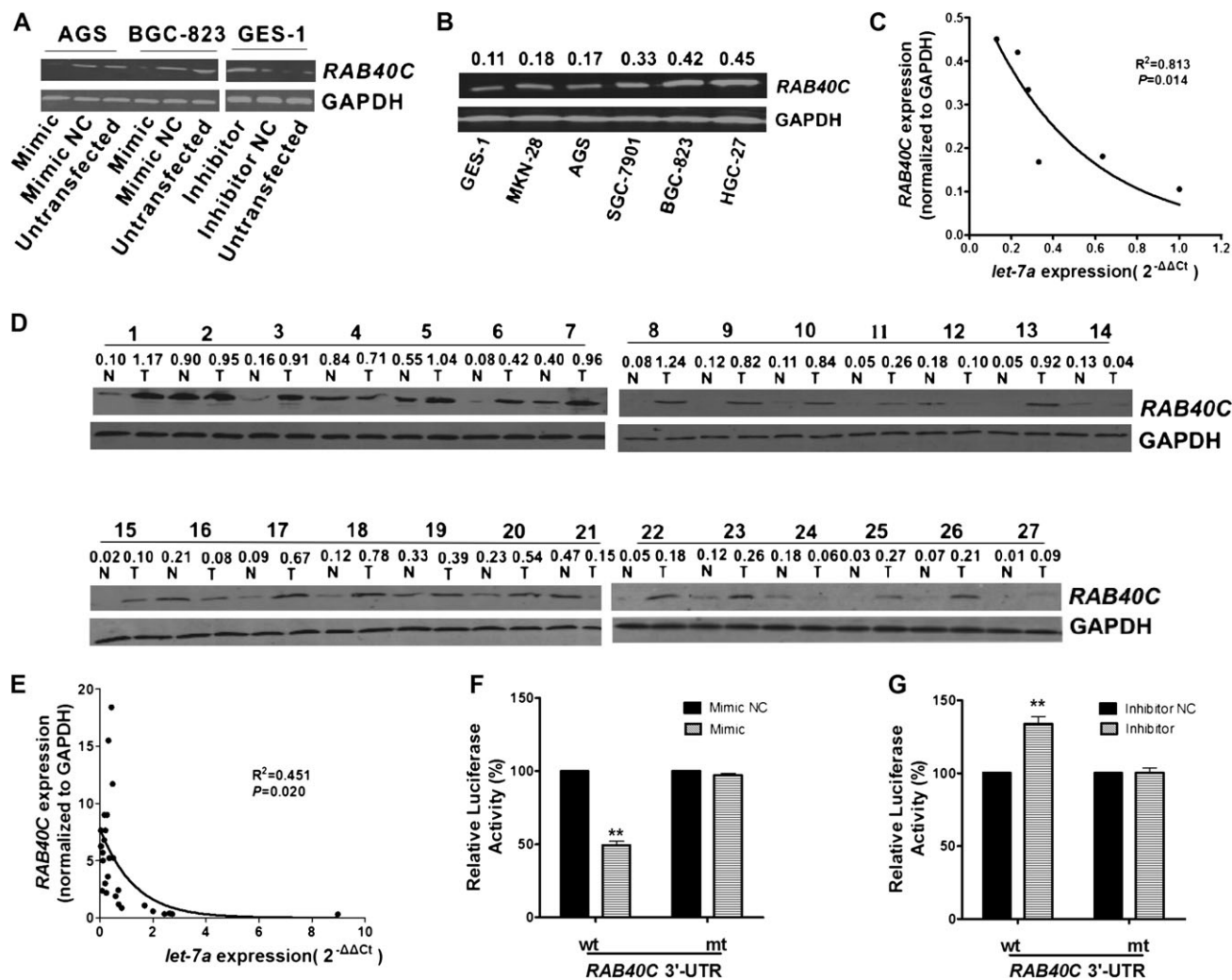


Fig. 5. *let-7a* negatively regulates *RAB40C* by binding to the *RAB40C* 3'-UTR. (A) *let-7a* mimic reduced *RAB40C* protein in AGS and BGC-823 cells and *let-7a* inhibitor increased *RAB40C* protein levels in GES-1 cells. (B–C) Analysis of the protein expression levels of *RAB40C* and correlation with *let-7a* expression in five gastric cancer cell lines and the GES-1 cell line. Protein expression was determined by western blotting (B). The expression of *let-7a* is plotted against protein expression (C). Coefficient of determination from logarithmic regression model (R^2) and P values are given ($R^2 = 0.813$; $P = 0.014$). (D–E) Analysis of the protein expression levels of *RAB40C* and correlation with *let-7a* expression in 27 pairs of gastric cancer tissues and matched normal gastric tissues. Protein expression was determined by western blotting (D) and the expression of *let-7a* is plotted against protein expression (E). Coefficient of determination from logarithmic regression model (R^2) and P values are given ($R^2 = 0.451$; $P = 0.020$). The value on each lane in (B and D) indicates the relative expression level of *RAB40C*, which is represented by the intensity ratio between *RAB40C* and glyceraldehyde-3-phosphate dehydrogenase fragments in each lane. (F–G) Analysis of luciferase activity. *let-7a* mimic (F) or inhibitor (G) inhibited or enhanced wild type but not mutant *RAB40C* 3'-UTR reporter activity. ** $P < 0.01$, compared with the mimic or inhibitor NC group. P values were obtained by two-tailed Student's t -test. Each reporter plasmid was transfected at least twice (on different days), and each sample was assayed in triplicate.

transcripts, with a total of 905 conserved binding sites and 125 poorly conserved binding sites. *RAB40C* is a member of the *RAS* family, which plays important roles in the regulation of immune responses, embryo and cell lineage development, cell cycle progression, inflammation and oncogenesis and is involved in the execution of important steps in tumorigenesis (36,37). Moreover, the dysregulation of *RAS* family members is frequently observed in human cancers (38–40). In this study, *RAB40C* was significantly overexpressed in gastric tumor samples compared with the matched normal tissue. Based on the bioinformatic analysis, *let-7a* binds to the 3'-UTR of *RAB40C* mRNA with lower free energy than *N-Ras* mRNA. It might stabilize a favorable conformation that facilitates the binding between *let-7a* and 3'-UTRs of *RAB40C* (41,42), which prompted us to explore whether *RAB40C* is a functional target of *let-7a*.

Here, we demonstrate that *RAB40C* is regulated directly by *let-7a*. This is evident at the level of the *RAB40C* protein is dysregulated by the change of *let-7a* expression without any change in the amount of

RAB40C mRNA. In addition, there was a significant inverse correlation of *let-7a* expression with the level of *RAB40C* protein in gastric cancer cell lines and gastric tumor tissues. To the best of our knowledge, this is the first report showing a correlation between *RAB40C* mRNA and *let-7a* miRNA in clinical samples of human cancer. Moreover, mutation of the *let-7a*-binding site abolished the effect of *let-7a* on the regulation of *RAB40C* fluorescence intensity. Importantly, depletion of *RAB40C* by siRNA transfection partly rescues the reduced cellular proliferation and the plating efficiency of cells in soft agar observed upon *let-7a* up-regulation, further demonstrating that *RAB40C* is a target of *let-7a* and suggesting an essential role for *RAB40C* as a mediator of the biological effects of *let-7a* in gastric tumorigenesis. This is the first study to show that *RAB40C* is negatively regulated by *let-7a* at the posttranscriptional level via binding to the 3'-UTR of *RAB40C* mRNA in gastric cancer cells.

In summary, we report that *let-7a* expression was decreased in human gastric cancer tissues and cell lines. Our study extended the

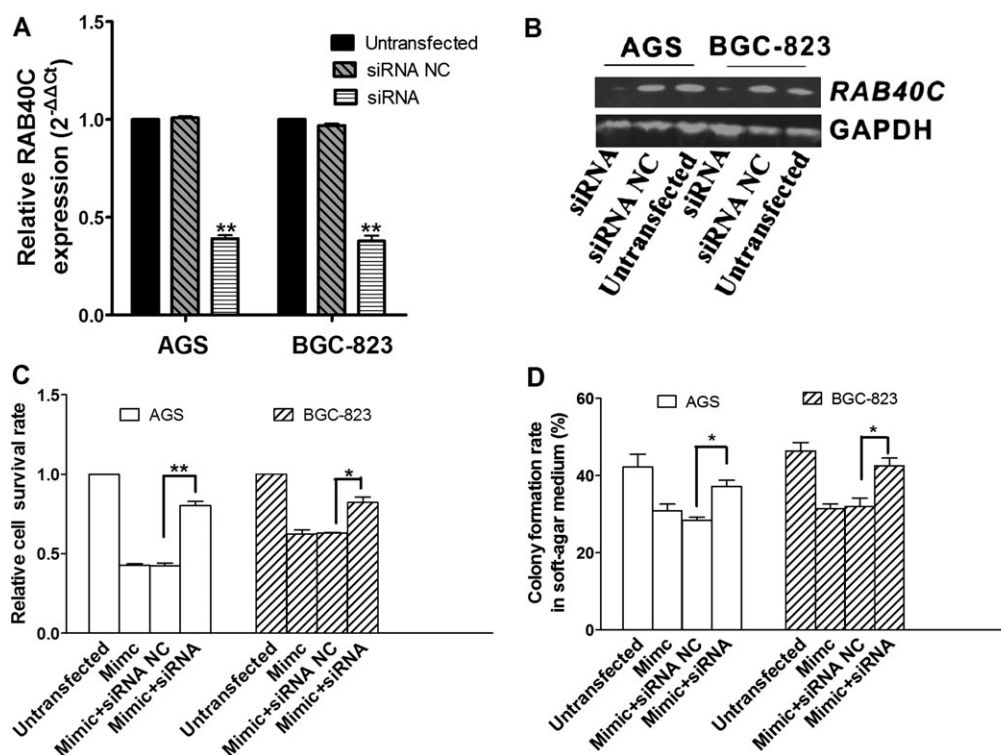


Fig. 6. The effect of *RAB40C* siRNA and *let-7a* mimic on cell proliferation and anchorage-independent growth. (A) Suppression of *RAB40C* mRNA expression levels by *RAB40C* siRNA transfection. (B) Suppression of *RAB40C* protein expression levels by *RAB40C* siRNA transfection. (C) The effect of *RAB40C* siRNA and *let-7a* mimic on cell proliferation. Relative cell growth is compared with the untransfected group. (D) The effect of *RAB40C* siRNA and *let-7a* mimic on anchorage-independent growth of cells. Data are given as mean \pm SD from three independent experiments. * $P < 0.05$; ** $P < 0.01$, compared with the siRNA NC group. P values were obtained by one-way analysis of variance or the non-parametric Kruskal–Wallis H test for multiple comparisons.

impact of *let-7a* to gastric cancer by showing for the first time that *let-7a* decreased proliferation and cell cycle in gastric cancer cells and inhibited tumor growth in nude mice. These effects are possibly due to down-regulation of *RAB40C* by *let-7a*. Therefore, miRNAs, in particular *let-7a*, might serve as potentially useful targets for gastric cancer diagnosis and therapy. Future studies will be aimed at developing strategies to use *let-7a* and *RAB40C* as a therapeutic regimen.

Supplementary material

Supplementary Figures S1–S4 can be found at <http://carcin.oxfordjournals.org/>

Funding

National Natural Science Foundation of China (30771780, 30972443 to J.Y.); Natural Science Foundation of Guangdong Province (07117550, 9251018201000004 to J.Y.); Science and Technology Program of Guangzhou Bureau of Education (08A093 to J.Y., 08A092 to Y.Q.); Science and Technology Pillar Program of Jiangxi Province (2009zDS16000 to C.H.).

Acknowledgements

We thank Xin Zhou and Wei Li (Department of General Surgery, First Affiliated Hospital of Nanchang University) for collecting the clinicopathologic information for the patients. We thank Rong Liu (Institute of Respiratory Diseases, First Affiliated Hospital of Guangzhou Medical University) for assistance with the nude mice assays.

Conflict of Interest Statement: None declared.

References

1. Parkin, D.M. *et al.* (2005) Global cancer statistics, 2002. *CA Cancer J. Clin.*, **55**, 74–108.

2. Yang, L. *et al.* (2005) Estimates of cancer incidence in China for 2000 and projections for 2005. *Cancer Epidemiol. Biomarkers Prev.*, **14**, 243–250.
3. Ambros, V. (2004) The functions of animal microRNAs. *Nature*, **431**, 350–355.
4. Engels, B.M. *et al.* (2006) Principles and effects of microRNA-mediated post-transcriptional gene regulation. *Oncogene*, **25**, 6163–6169.
5. Lim, L.P. *et al.* (2005) Microarray analysis shows that some microRNAs downregulate large numbers of target mRNAs. *Nature*, **433**, 769–773.
6. Lewis, B.P. *et al.* (2005) Conserved seed pairing, often flanked by adenosines, indicates that thousands of human genes are microRNA targets. *Cell*, **120**, 15–20.
7. Hwang, H.W. *et al.* (2006) MicroRNAs in cell proliferation, cell death, and tumorigenesis. *Br. J. Cancer*, **94**, 776–780.
8. Alvarez-Garcia, I. *et al.* (2005) MicroRNA functions in animal development and human disease. *Development*, **132**, 4653–4662.
9. Krutzfeldt, J. *et al.* (2006) Strategies to determine the biological function of microRNAs. *Nat. Genet.*, **38**, S14–S19.
10. Calin, G.A. *et al.* (2004) Human microRNA genes are frequently located at fragile sites and genomic regions involved in cancers. *Proc. Natl Acad. Sci. USA*, **101**, 2999–3004.
11. Iorio, M.V. *et al.* (2005) MicroRNA gene expression deregulation in human breast cancer. *Cancer Res.*, **65**, 7065–7070.
12. Calin, G.A. *et al.* (2005) A MicroRNA signature associated with prognosis and progression in chronic lymphocytic leukemia. *N. Engl. J. Med.*, **353**, 1793–1801.
13. Yanaihara, N. *et al.* (2006) Unique microRNA molecular profiles in lung cancer diagnosis and prognosis. *Cancer Cell*, **9**, 189–198.
14. Zhang, Z. *et al.* (2008) MiR-21 plays a pivotal role in gastric cancer pathogenesis and progression. *Lab. Invest.*, **88**, 1358–1366.
15. Liu, T. *et al.* (2008) MicroRNA-27a functions as an oncogene in gastric adenocarcinoma by targeting prohibitin. *Cancer Lett.*, **273**, 233–242.
16. Petrocca, F. *et al.* (2008) E2F1-regulated microRNAs impair TGFbeta dependent cell-cycle arrest and apoptosis in gastric cancer. *Cancer Cell*, **13**, 272–286.
17. Xia, L. *et al.* (2008) miR-15b and miR-16 modulate multidrug resistance by targeting BCL2 in human gastric cancer cells. *Int. J. Cancer*, **123**, 372–379.

18. Du, Y. *et al.* (2009) Down-regulation of miR-141 in gastric cancer and its involvement in cell growth. *J. Gastroenterol.*, **44**, 556–561.
19. Bandres, E. *et al.* (2009) MicroRNA-451 regulates macrophage migration inhibitory factor production and proliferation of gastrointestinal cancer cells. *Clin. Cancer Res.*, **15**, 2281–2290.
20. Takagi, T. *et al.* (2009) Decreased expression of microRNA-143 and -145 in human gastric cancers. *Oncology*, **77**, 12–21.
21. Luo, H. *et al.* (2009) Down-regulated miR-9 and miR-433 in human gastric carcinoma. *J. Exp. Clin. Cancer Res.*, **16**, 28–42.
22. Takamizawa, J. *et al.* (2004) Reduced expression of the let-7 microRNAs in human lung cancers in association with shortened postoperative survival. *Cancer Res.*, **64**, 3753–3756.
23. Akao, Y. *et al.* (2006) let-7 microRNA functions as a potential growth suppressor in human colon cancer cells. *Biol. Pharm. Bull.*, **29**, 903–906.
24. Johnson, S.M. *et al.* (2005) RAS is regulated by the let-7 microRNA family. *Cell*, **120**, 635–647.
25. Sampson, V.B. *et al.* (2007) MicroRNA let-7a downregulates MYC and reverts MYC-induced growth in Burkitt lymphoma cells. *Cancer Res.*, **67**, 9762–9770.
26. Mayr, C. *et al.* (2007) Disrupting the pairing between let-7 and HMGA2 enhances oncogenic transformation. *Science*, **315**, 1576–1579.
27. Motoyama, K. *et al.* (2008) Clinical significance of high mobility group A2 in human gastric cancer and its relationship to let-7 microRNA family. *Clin. Cancer Res.*, **14**, 2334–2340.
28. Pfaffl, M.W. (2001) A new mathematical model for relative quantification in real-time RT-PCR. *Nucleic Acids Res.*, **29**, e45.
29. Si, M.L. *et al.* (2007) miR-21-mediated tumor growth. *Oncogene*, **26**, 2799–2803.
30. Long, X.B. *et al.* (2009) Let-7a microRNA functions as a potential tumor suppressor in human laryngeal cancer. *Oncol. Rep.*, **22**, 1189–1195.
31. Shell, S. *et al.* (2007) Let-7 expression defines two differentiation stages of cancer. *Proc. Natl Acad. Sci. USA.*, **104**, 11400–11405.
32. Johnson, C.D. *et al.* (2007) The let-7 microRNA represses cell proliferation pathways in human cells. *Cancer Res.*, **67**, 7713–7722.
33. Schlüter, C. *et al.* (1993) The cell proliferation-associated antigen of antibody Ki-67: a very large, ubiquitous nuclear protein with numerous-repeated elements, representing a new kind of cell cycle-maintaining proteins. *J. Cell Biol.*, **123**, 513–522.
34. Bandres, E. *et al.* (2007) MicroRNAs as cancer players: potential clinical and biological effects. *DNA Cell Biol.*, **26**, 273–282.
35. Su, H. *et al.* (2009) MicroRNA-101, down-regulated in hepatocellular carcinoma, promotes apoptosis and suppresses tumorigenicity. *Cancer Res.*, **69**, 1135–1142.
36. Ng, E.L. *et al.* (2008) Rab GTPases and their roles in brain neurons and glia. *Brain Res. Rev.*, **58**, 236–246.
37. Rodriguez-Gabin, A.G. *et al.* (2004) Vesicle transport in oligodendrocytes: probable role of Rab40c protein. *J. Neurosci. Res.*, **76**, 758–770.
38. Chen, X. *et al.* (2009) Role of miR-143 targeting KRAS in colorectal tumorigenesis. *Oncogene*, **28**, 1385–1392.
39. Leung, P.S. (2010) Current research of the RAS in pancreatitis and pancreatic cancer. *Adv. Exp. Med. Biol.*, **690**, 179–199.
40. Cortot, A.B. *et al.* (2010) KRAS mutation status in primary nonsmall cell lung cancer and matched metastases. *Cancer*, **116**, 2682–2687.
41. Lindow, M. *et al.* (2007) Principles and limitations of computational microRNA gene and target finding. *DNA Cell Biol.*, **26**, 339–351.
42. Rehmsmeier, M. *et al.* (2004) Fast and effective prediction of microRNA/target duplexes. *RNA*, **10**, 1507–1517.

Received September 29, 2010; revised January 21, 2011;
accepted February 12, 2011